International Journal of Engineering Advanced Research
eISSN: 2710-7167 | Vol. 4 No. 3 [September 2022]
Journal website: http://myjms.mohe.gov.my/index.php/ijear

DETERMINING THE ELASTIC PROPERTIES OF FLEXIBLE 3D PRINTED BEAMS WITH VARIABLE INFILL DENSITIES AND PATTERNS

Anirudha Bhattacharjee[1*], Pancho Dachkinov[2], Hiroaki Wagatsuma[3] and Bishakh Bhattacharya[4]

[1 4] Department of Mechanical Engineering, Indian Institute of Technology Kanpur, Kanpur, INDIA

[2 3] Graduate School of Life Science and Systems Engineering, Kyushu Institute of Technology, Kitakyushu, JAPAN

*Corresponding author: anirub@iitk.ac.in

Article Information:

Article history:

Received date	: 1 July 2022
Revised date	: 25 July 2022
Accepted date	: 1 September 2022
Published date	: 7 September 2022

To cite this document:

Bhattacharjee, A., Dachkinov, P., Wagatsuma, H., & Bhattacharya, B. (2022). DETERMINING THE ELASTIC PROPERTIES OF FLEXIBLE 3D PRINTED BEAMS WITH VARIABLE INFILL DENSITIES AND PATTERNS. *International Journal of Engineering Advanced Research*, *4*(3), 12-24.

Abstract: *Flexible non-linear 3D printed materials are rapidly gaining popularity in various engineering applications such as soft robotics, actuators, medical devices, etc. Due to their wide applicability, there is an increased research interest in characterization of their mechanical properties and performance. Unlike the conventional manufacturing processes, 3D printing has an additive character and allows for the geometry to be controlled from inside. The internal geometry and density corresponding to a given model can be tuned to a desired stiffness. In this study we investigate the effect of the infill percentage and infill geometry on the mechanical properties of 3D printed samples from flexible material by using a desktop type FDM 3D printer. The analyzed samples have the same shape and geometry – a beam with a square cross-section but the infill percentage is varied from 10 % to a 100 % with an increment of 15 %. The effects of three different types of infill geometries– rectangular, square and honeycomb have also been analytically determined. The approach for the analytical formulation adopts the methodology for calculating the in-plane properties and stiffnesses in cellular solids. The results for the mechanical properties for the different infill densities and infill geometries have been compared for all configurations. Despite the common external geometry of all beams, there is a significant change in their stiffness*

with the variation of the infill patterns and densities. Finally, a non-linear FEA study for the fully solid beam was conducted and compared with the analytical results. The method, used in this study can be applied for optimization of the stiffness to weight ratio during the design process of flexible 3D printed parts undergoing larger deformations.

Keywords: 3D printing, flexible materials, infill geometry, infill density, cellular solids, non-linear FEA.

1. Introduction

3D Printing in all its variations has become accessible and affordable technology in the recent years. That can be explained by the constant improvements of the process and filaments.

The increased interest is mainly due to the capabilities of 3D Printing as an appropriate technology for fabricating complex geometry. Some of the unique characteristics of the process are:

- Ability to create hollow parts from inside.
- Fabricating parts with variable structure from the inner volume – infill pattern and density.
- Cost-efficient benefits – there are no tools required; the price of the components depends less on their complexity and more from the printing time and material usage.
- Environmentally friendly process – there are no wasted materials some of the materials from failed parts could be recycled.

3D Printing is used for creating not only prototypes but functional parts as well due to its unique capabilities of fabricating the models by adding layers of material instead of the conventional technologies - by removing material. To achieve such implementation, the mechanical properties of the materials are crucial.

The variety of materials is growing fast, and researchers have focused their attention to investigate the quality of these filaments. In addition to the materials, the process of 3D printing being additive in its nature, allows for unique specific techniques to be applied such as control of the infill density and infill geometry from inside of the model – a property unavailable to the traditional manufacturing processes. To better optimize the design of a model, all the above parameters have to be considered. Some of the 3D Printing capabilities have already been investigated due to its growing popularity. However, it is important to note that the results of these studies can vary depending on the printer type and materials which significantly influence the mechanical properties and quality of the parts.

The rest of this article is structured as follows: Section II gives the research background, the Methodologies for determining elastic coefficient are described in Section III, Section IV explains the experimental setup that has been developed, Section V summarizes the results, VI gives a discussion and Section VII concludes the paper.

2. Literature Review

One of the most spread materials is Poly Lactic Acid (PLA). This a relatively low cost and environmentally friendly filament used by the FDM (Fused Deposition Modeling) 3D Printers. The mechanical properties of this material are explored at a tensile and flexural tests by (Catana, Pop, & Brus, 2021). PLA has been compared with other popular 3D Printing filaments such as ABS (Acrylonitrile Butadiene Styrene) by (Ahmed et al., 2016; Brčić, Kršćanski, & Brnić, 2021). Other works investigate the relative density of flexible cellular structures fabricated from TPU (thermoplastic polyurethane) filament (Płatek et al., 2020). Effects of the infill density within a monolith part on the mechanical behavior of tensile tests for several different filament types have also been covered in (Johnson & French, 2018). In addition to the tensile stress analysis, some studies such as (Alvarez C, Lagos C, & Aizpun, 2016) also investigate the printing time and the impact resistance of the models. Researchers have also conducted experiments where the infill geometry of the samples is varied (Fernandez-Vicente, Calle, Ferrandiz, & Conejero, 2016; Galeta, Raos, Stojšić, & Pakši, 2016). In some cases the infill orientation and its influence on the parts performance is explored on bending and tensile stress tests (Letcher & Waytashek, 2014). The infill geometry has been investigated in terms of relationship between loading conditions and printing costs in (Baich & Manogharan, 2015). Some studies investigate both the infill percentage (density) and infill geometry (pattern) (Farbman & McCoy, 2016). Finally, there are works that have developed a new types and variations of 3D Printing materials especially TPU (Xiao & Gao, 2017).

Determining the properties and the performance of the 3D printing filaments is necessary to optimize the parts. 3D Printing as an Additive Manufacturing process is suitable for fabricating Compliant Mechanisms. Compliant Mechanisms are single printed mechanisms where the entire process of assembling is avoided. That leads to frictionless parts where no heat and clearances are generated due to the friction between the components. These types of mechanisms rely solely on the deformation the execute the motion. They can be precisely controlled if the characteristics of the materials are known and therefore, better understanding of the filament's quality will allow more reliable design of Compliant Mechanisms and will expand their applications in the future.

The properties of the Compliant Mechanisms (Compliant Joints) are analyzed by (Liu, Bi, Yang, & Wang, 2014; Trease, Moon, & Kota, 2005). The methodology of designing such mechanisms is provided in (Ion, Lindlbauer, Herholz, Alexa, & Baudisch, 2019; Megaro et al., 2017).

2.1 Problem Statement

Stiffness of 3D printed parts are very hard to determine due to the variation in the internal geometry of various infill patterns. This can only be obtained experimentally and there is limited approach to systematically derive the mechanical properties analytically. Controlling the internal structure allows optimizing the desired stiffness to mass ration for 3D printed parts. In this work we derive

and compare the mechanical properties of three different infill patterns and seven different infill densities.

3. Method

Table 1 illustrates all possible combinations of infill patterns and densities that were compared in this study.

Table 1: Combinations of Infill Density and Infill Patterns

Infill Pattern / Infill Density, %	Triangular	Grid/Rectangular	Hexagonal/Tri-hexagon
10	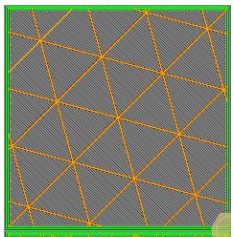	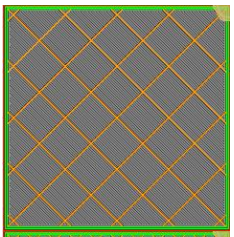	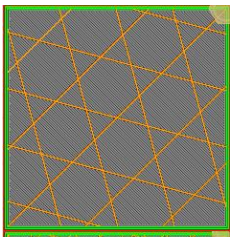
25	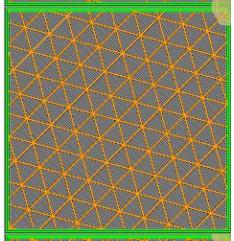	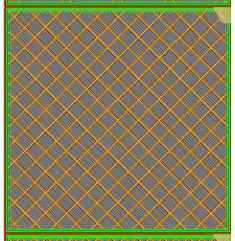	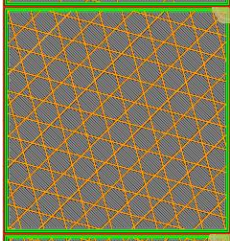
40	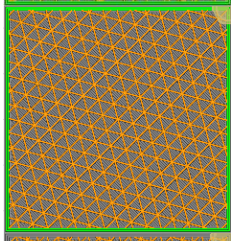	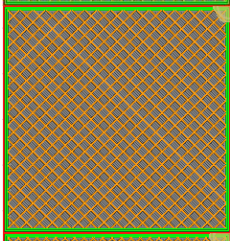	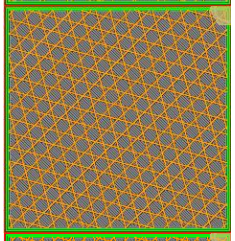
55	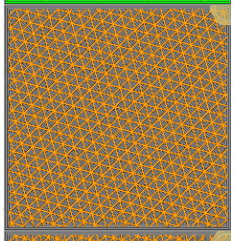	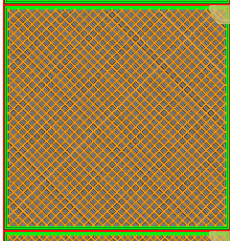	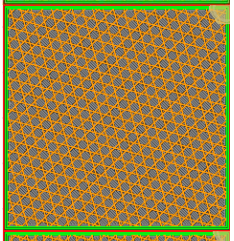
70	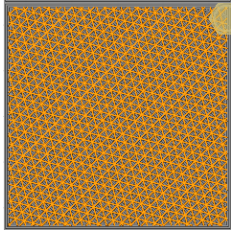	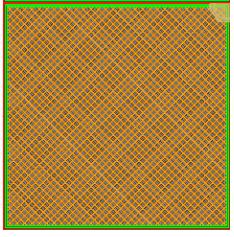	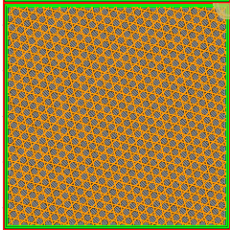

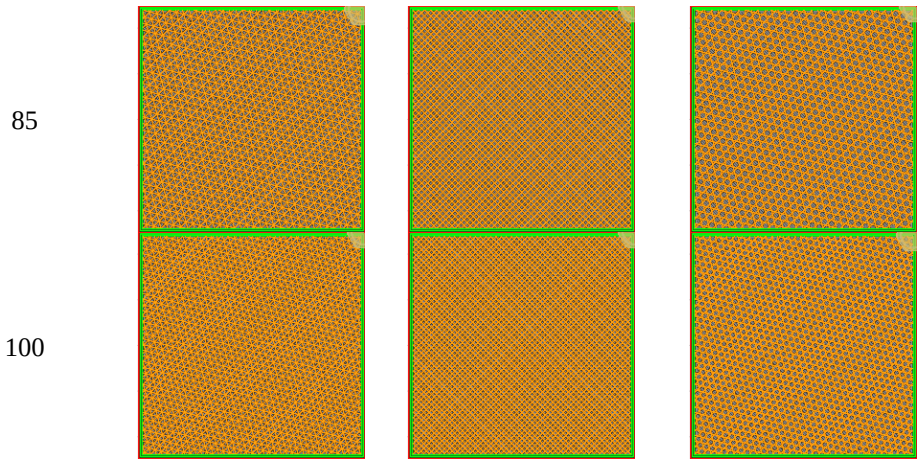

3.1 Flexible 3D Printed Samples and Printing Parameters

As discussed above, beams, fabricated from a flexible 3D Printing filament were designed with variable infill density – from 10% to 100% with step of 15% as shown on Figure 1.

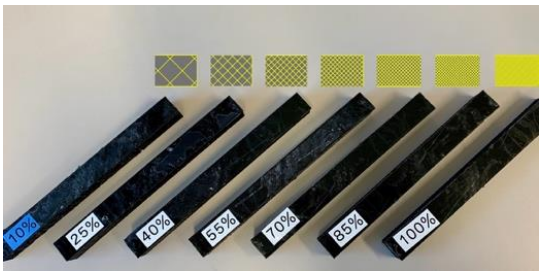

Figure 1: 3D Printing Samples with Variable Infill Density

The samples were designed in Autodesk Inventor Professional 2021. For preparing the models for 3D Printing, a slicing software Ultimaker Cura. The 3D Printing parameters are shown in Table 2. The 3D Printer is Anycubic i3 Mega. The flexible TPU materials is Ninja Flex from a company called NinjaTek (Ninjatek, 2022, June 22). This material is flexible in nature and is chosen due to its mechanical properties. The nozzle temperature settings were used as recommended by the manufacturer and shown in the table 2 is 230 ℃. The pattern of the infill is grid – described by Ultimaker Cura as 2D strong infill (Ultimaker, 2022, June 22).

Table 2: 3D Printing Parameters for the Samples

Parameter	Value
3D Printer	Anycubic i3 Mega
Slicing Software	Ultimaker Cura
3D Printing Material	Ninjatek Ninja Flex TPU Filament
Printing Temperature [℃]	230
Platform Temperature [℃]	60
Supporting Material	No
Infill Density, %	10, 25, 40, 55, 70, 85, 100
Infill Type	Grid
Layer Height, [mm]	0.15
Printing Speed, [mm/s]	50

3.2 Defining the Modulus of Elasticity for the Different Infill Geometries and Densities

3.2.1 Infill Pattern

Infill patterns (geometries), explored in this research and available in Ultimaker Cura are represented as cellular solids (technology, 2022, June 22). The infill types, generated by the slicing software are shown on Figure 2.

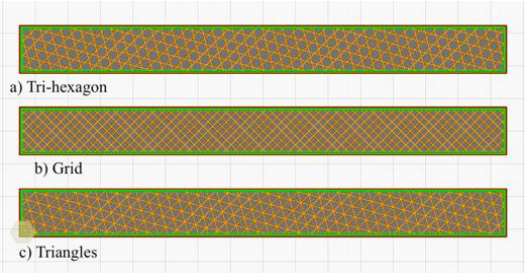

Figure 2: Infill Geometries in the Slicing Software

International Journal of Engineering Advanced Research
eISSN: 2710-7167 | Vol. 4, No. 3, 12-24, 2022
http://myjms.mohe.gov.my/index.php/ijear

To analyse the various patterns, they have been modelled as cellular solids as illustrated on Figure 3.

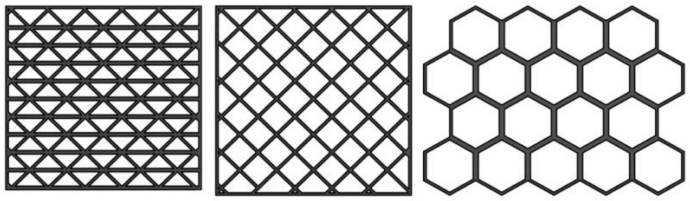

Figure 3: Modeling the Infill Patterns as Cellular Solids

The parameters of a single cell for all types of infill as well as the deformations are shown on Figure 4.

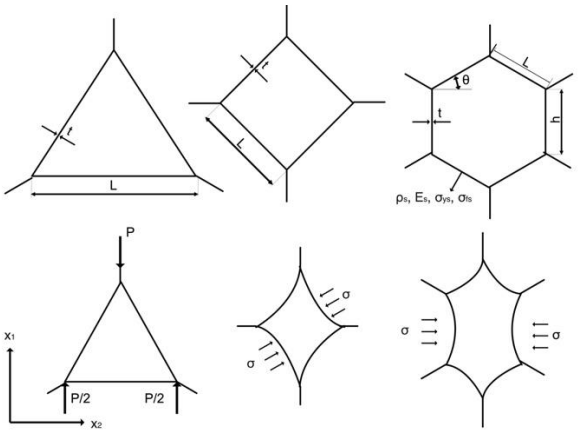

a) triangular b) rectangular c) honeycomb cell

Figure 4: Parameters of the Cells

Figure 4 shows common cell types of cellular solids also used in this work to model the infill patterns. Triangular cells shown on Figure 4 a), the following characteristics:

- Behave like a truss.
- Analysed as pin joints (no moments at the nodes).
- Only axial loads along the members.
- Forces in each member are proportional to P.

$$E^* \propto \frac{P}{b}\frac{E_s bt}{Pl} = CE_s\left(\frac{t}{l}\right) \quad (1)$$

where: C is a constant related with the cell geometry, for equilateral triangle, C=1.15.
Figure 4 b) shows rectangular cells that represent the grid infill type.
Those in the diagonal direction, called E^*_{45}, are given by:

$$E^*_{45} = 2E_s\left(\frac{t}{l}\right)^3 \quad (2)$$

The Young's modulus can be obtained from the limit of the equations for hexagonal cells when h= 0 and θ= 45°.

On Figure 4 c) are shown regular hexagonal cells. The modulus of elasticity for that type of cells can be obtained by the following equation:

$$E_1^* = E_s \left(\frac{t}{l}\right)^3 \cdot \frac{cos\theta}{(h/l+sin\theta)sin^2\theta} \quad (3)$$

where:

- Properties of the solid: Young's Modulus of the solid E_s;
- $\left(\frac{t}{l}\right)^3$ related to the relative density (volume fraction of the solid).
- $(h/l + sin\theta)sin^2\theta$ factor that depends on cells geometry.

For regular hexagonal honeycomb: $\frac{h}{l} = 1;\ \theta = 30°$.:

$$E_1^* = \frac{4}{\sqrt{3}} E_s \left(\frac{t}{l}\right)^3 \quad (4)$$

3.2.2 Infill Density

Infill density of the beams is a parameter related to the relative density.

- Density of the cellular material, ρ^*;
- Density of the solid material, ρ_s.

$$\frac{\rho^*}{\rho_s} = \frac{M_s}{V_t} \cdot \frac{V_s}{M_s} = \frac{V_s}{V_t} = \frac{\left(\frac{t}{l}\right)\left(\frac{h}{l}+2\right)}{2cos\theta\left(\frac{h}{l}+\sin\theta\right)} \quad (5)$$

where: M_s is the mass of the solid, V_t and V_s are the total volume and the volume of the solid respectively.

3.3 Volume Related Parameters:

To determine the volume of the solid V_s each, beam the following 3D Printing limitations have to be considered:

1. Calculating the volume of the shell (the side walls and top and bottom layers) made out of solid material (100% infill);
2. Layer thickness.
3. Top and bottom layer thickness.
4. Least thickness for the top and bottom layers.
5. Number of the top and bottom layers (layer thickness divided by the layer height).
6. Diameter of the nuzzle (theoretically, the thinnest layer can be printed with the diameter of the nuzzle).
7. Wall thickness (side walls of the model).

The stiffness is calculated in (6). It is a function of the Elasticity E and the strain ε.

$$\sigma_1 = E\varepsilon = \frac{P}{A} = \frac{P}{(h+lsin\theta)b} \quad (6)$$

where: *P* is the applied loading, *A* is the area on which the load is applied; *b* is the thickness of the 3D printed layer. The strain in the samples is expressed by (7).

$$\varepsilon_1 = \frac{\delta sin\theta}{lcos\theta} \tag{7}$$

$$\delta = \frac{(2)Psin\theta(^l/_2)^3}{3E_sI} = \frac{Psin\theta l^3}{12E_sI} \tag{8}$$

$$I = \frac{bt^3}{12} \tag{9}$$

where: δ is the deflection of the sample; *l* is the length of the side of the sample (shown on Figure 4); E_s is the Modulus of Elasticity of the material; *I* is the moment of inertia.

4. Results and Discussion

4.1 Analytical Results

To determine the geometrical constraints of the beam, the below parameters are used:

1. Material: Ninjatek Ninjaflex TPU filament.
2. Square cross-section of a= 0.015 m and length l= 0.15 m.
3. Layer thickness (equal to the depth b): 0.15 mm.
4. Top layer thickness: 1.2 mm.
5. Bottom layer thickness: 1.2 mm.
6. Number of the top and bottom layers: 8.
7. Diameter of the nozzle (equal to the thickness of the wall): 0.3 mm.
8. Wall thickness: 1.2 mm.

After solving (5) for the relative density and $\frac{t}{l}$, if $\frac{h}{l} = 1$ and E of the material is 12 MPa, for triangular cells (patterns) $\theta = 60°$; for rectangular - $\theta = 45°$; for hexagonal - $\theta = 30°$, the results for the Elasticity for the 3 types of infill and 7 densities are calculated. The applied loading, used for the analytical part as well as the FEA analysis is 5 N.

Figure 5 a) shows parameters affected by the infill percentage directly. All samples are printed with the same regimes. After, the 3D printing time and the mass of the completed specimens is measured. As it can be observed, the duration of the printing process is increasing in a linear fusion up until 90% but gets significantly higher (more than 2 times) for 100% infill. Similarly, the mass of the models and their density progresses linearly to 90% and the increase from 90% to a 100% is with a greater increment. Therefore, to save time and materials and to make the parts lighter, it can be recommended for models with only visual value to be printed with infill percentages lower than a 100%.

As expected, on Figure 5 b) the relative elasticity of the samples increases with the increase of the infill. In addition, it was also expected that the highest values will be for the triangular infill pattern due to the parameter $\frac{t}{l}$ related to the relative density (volume fraction of the solid). The volume

fraction of the solid for rectangular and hexagonal infill patterns is raised on the third power which leads to lower values of their elasticity moduli. However, that is not the case because with the increase of the infill density, length *l* (illustrated on Figure 4 and used in equation (8) to calculate the deflection) is decreasing. This is due to the fact that more cells have to fit in a given volume by increasing the infill density and the only way is by making the cells smaller (smaller *l*).

On Figure 6 a) the values of the strain are shown. As expected with the increase of the infill, the strain decreases which makes the parts produced with higher infill density stiffer. Here, the highest strain values are for the triangular infill pattern and the highest – for the hexagonal. Similar trend can be observed for the stiffness. It raises with the infill density and is the highest for the hexagonal pattern (Figure 6 b)).

4.1 Finite Element Analysis Results

FEA simulation was conducted on a beam of similar dimension and mechanical properties of Ninja Flex was used as given in manufacturer specification. The simulation study was conducted in COMSOL and the stresses and displacements co-responding to a tip load is illustrated in Figure 7. The non-linear behaviour of the beam can be seen in figure 7 b) where the load has been varied from 0.5 N to 5 N with an interval of 0.5 N. The FEA analysis aims to represent the stress for a beam with 100% infill density. The results of the deformation from this study for 5 N force are 0.075 mm are similar to the values of the deflection for 100% infill density and rectangular pattern – 0.0704 mm.

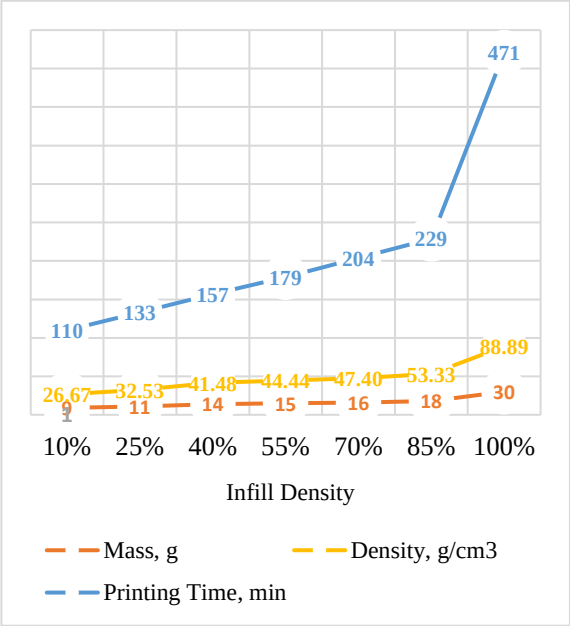

(a) Impact of the Infill Density on the 3D Printing Parameters

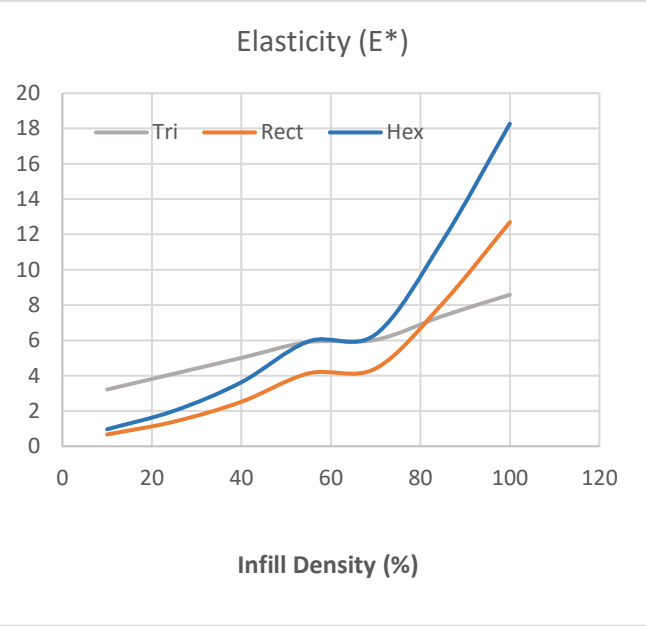

(b) Relative Density-Modulus of Elasticity Relationship

Figure 5: Impact of Infill-Density on 3D Printing Parameters and Modulus of Elasticity (Analytical).

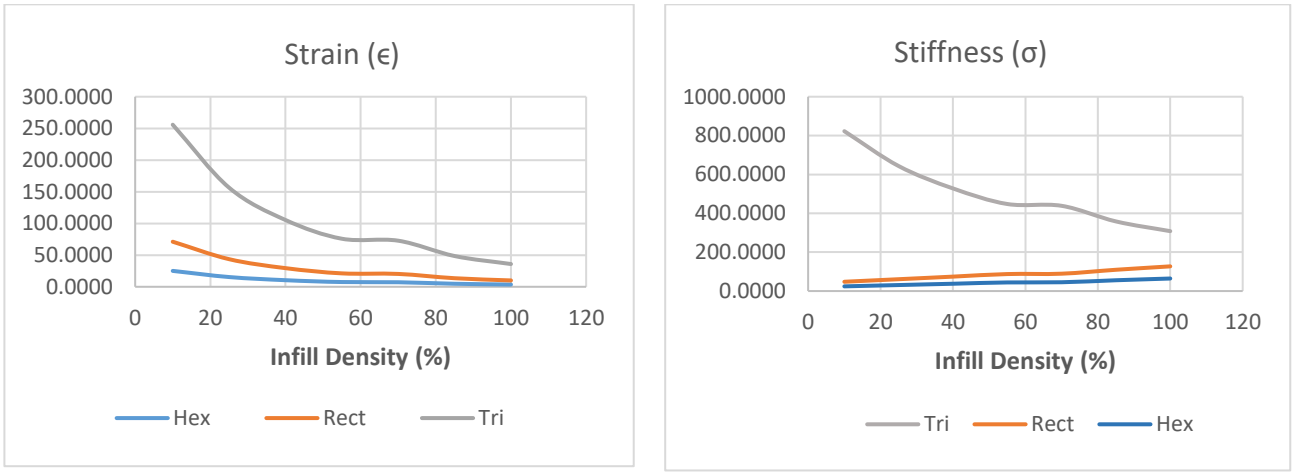

a) Strain b) Stiffness

Figure 6: Impact of Infill-Density on 3D Printing Parameters and Modulus of Elasticity (Analytical).

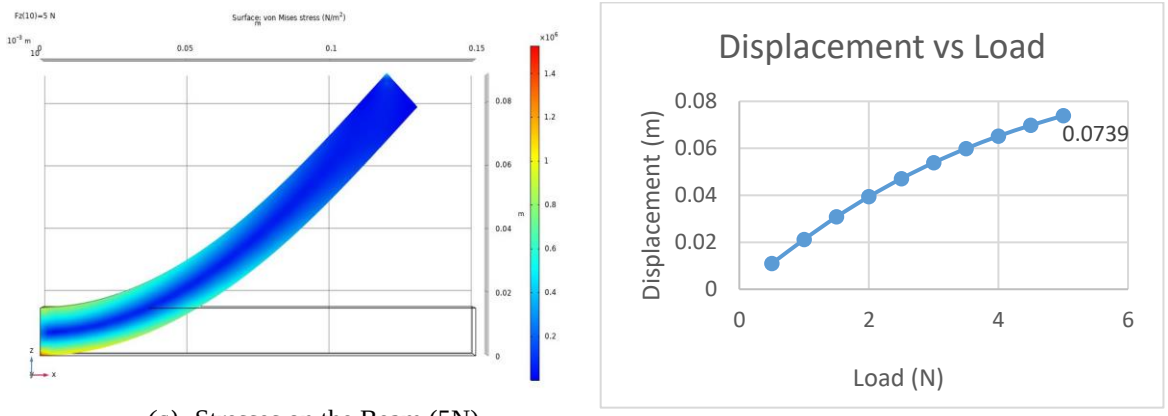

(a) Stresses on the Beam (5N) *(b)* Displacements of the tip (0.5N – 5N)

Figure 7: Stresses and Displacements of the Beam from COMSOL FEA Analysis

5. Conclusion

In this study we investigate the influence of the infill patterns and infill densities on the mechanical properties of samples fabricated from flexible TPU filament by implementing the cellular solid model. The results are obtained analytically for 3 common types of infill geometries – triangular, rectangular, and hexagonal and for 7 infill percentages – 10, 25, 40, 55, 70, 85 and 100. The values of the deflection, strain, elasticity, and stress for all 21 combinations are presented. The relative elasticity increases as the infill percentage increases and is the highest for the hexagonal infill pattern. The values for rectangular and triangular patterns are close to each other with lowest modulus of elasticity calculated for the triangular.

The values of the strain, as expected, with the increase of the infill, the strain decreases. The highest strain values are for the triangular infill pattern and the highest – for the hexagonal. Similarly, for the stiffness, it raises with the infill density and is the highest for the hexagonal pattern.

The deformation is compared to a non-linear FEA analysis for a beam from 100% infill density with the same properties of NinjaFlex filament. From the simulation is obvious that the deflection is close to the values for rectangular pattern with 100% infill.

It is important to note, that the results obtained analytically should be verified with an experimental data of beams fabricated from the same NinjaFlex material and parameters.

This methodology can be applied in the design process of flexible parts with controlled elasticity and optimized mass to stiffness ration while at the same time presenrving the outer geometry of the models.

6. Acknowledgement

This work was supported in part by the research project on "Bio-medical Instrumentation of Validated Human-Robot Interactions to Enhance Learning and Developmental Processes in Children" supported by the Department of Science and Technology (DST), Ministry of Science & Technology, Government of India, New Delhi and the Japan Society for the Promotion of Science (JSPS) in the form of the India-Japan Cooperative Science Programme (IJCSP) and the New Energy and Industrial Technology Development Organization (NEDO) and Project on Regional Revitalization Through Advanced Robotics (Kyushu Institute of Technology/Kitakyushu city, Japan).

References

Ahmed, M., Islam, M. R., Vanhoose, J., Hewavitharana, L., Stanich, A., & Hossain, M. (2016). *Comparisons of Bending Stiffness of 3D Printed Samples of Different Materials.* Paper presented at the ASME International Mechanical Engineering Congress and Exposition.

Alvarez C, K. L., Lagos C, R. F., & Aizpun, M. (2016). Investigating the influence of infill percentage on the mechanical properties of fused deposition modelled ABS parts. *Ingeniería e Investigación, 36*(3), 110-116.

Baich, L., & Manogharan, G. (2015). *Study of infill print parameters on mechanical strength and production cost-time of 3D printed ABS parts.* Paper presented at the 2014 International Solid Freeform Fabrication Symposium.

Brčić, M., Kršćanski, S., & Brnić, J. (2021). Rotating Bending Fatigue Analysis of Printed Specimens from Assorted Polymer Materials. *Polymers, 13*(7), 1020.

Catana, D., Pop, M.-A., & Brus, D.-I. (2021). Comparison between the test and simulation results for PLA structures 3D printed, bending stressed. *Molecules, 26*(11), 3325.

Farbman, D., & McCoy, C. (2016). *Materials testing of 3D printed ABS and PLA samples to guide mechanical design.* Paper presented at the International Manufacturing Science and Engineering Conference.

Fernandez-Vicente, M., Calle, W., Ferrandiz, S., & Conejero, A. (2016). Effect of infill parameters on tensile mechanical behavior in desktop 3D printing. *3D printing and additive manufacturing, 3*(3), 183-192.

Galeta, T., Raos, P., Stojšić, J., & Pakši, I. (2016). Influence of structure on mechanical properties of 3D printed objects. *Procedia Engineering, 149*, 100-104.

Ion, A., Lindlbauer, D., Herholz, P., Alexa, M., & Baudisch, P. (2019). *Understanding metamaterial mechanisms.* Paper presented at the Proceedings of the 2019 CHI Conference on Human Factors in Computing Systems.

Johnson, G. A., & French, J. J. (2018). Evaluation of infill effect on mechanical properties of consumer 3D printing materials. *Advances in Technology Innovation, 3*(4), 179.

Letcher, T., & Waytashek, M. (2014). *Material property testing of 3D-printed specimen in PLA on an entry-level 3D printer*. Paper presented at the ASME international mechanical engineering congress and exposition.

Liu, L., Bi, S., Yang, Q., & Wang, Y. (2014). Design and experiment of generalized triple-cross-spring flexure pivots applied to the ultra-precision instruments. *Review of Scientific Instruments, 85*(10), 105102.

Megaro, V., Zehnder, J., Bächer, M., Coros, S., Gross, M. H., & Thomaszewski, B. (2017). A computational design tool for compliant mechanisms. *ACM Trans. Graph., 36*(4), 82:81-82:12.

Ninjatek, N., Technical specifications. (2022, June 22). Ninjaflex 3d printer filament (85a). from https://ninjatek.com/shop/ninjaflex/#print-guidelines

Płatek, P., Rajkowski, K., Cieplak, K., Sarzyński, M., Małachowski, J., Woźniak, R., & Janiszewski, J. (2020). Deformation process of 3D printed structures made from flexible material with different values of relative density. *Polymers, 12*(9), 2120.

technology, M. i. o. (2022, June 22). Cellular solids: structure, properties and applications. from https://ocw.mit.edu/courses/3-054-cellular-solids-structure-properties-and-applications-spring-2015/pages/lecture-notes/

Trease, B. P., Moon, Y.-M., & Kota, S. (2005). Design of large-displacement compliant joints.

Ultimaker. (2022, June 22). Infill pattern. from https://support.ultimaker.com/hc/en-us/articles/360012607079-Infill-settings

Xiao, J., & Gao, Y. (2017). The manufacture of 3D printing of medical grade TPU. *Progress in Additive Manufacturing, 2*(3), 117-123.